PHYSICAL REVIEW C **77**, 047303 (2008)

# One-quasiparticle bands in neutron-rich $^{187}$W

T. Shizuma (静間俊行),[1] T. Ishii (石井哲朗),[2] H. Makii (牧井宏之),[2] T. Hayakawa (早川岳人),[1]
M. Matsuda (松田誠),[3] S. Shigematsu (重松宗一郎),[4] E. Ideguchi (井手口栄治),[5] Y. Zheng (鄭勇),[5]
M. Liu (柳敏良),[5] T. Morikawa (森川恒安),[6] and M. Oi (大井万紀人)[7]
[1]*Kansai Photon Science Institute, Japan Atomic Energy Agency, Kizugawa, Kyoto 619-0215, Japan*
[2]*Advanced Science Research Center, Japan Atomic Energy Agency, Tokai, Ibaraki 319-1195, Japan*
[3]*Department of Research Reactor and Tandem Accelerator, Japan Atomic Energy Agency, Tokai, Ibaraki 319-1195, Japan*
[4]*Department of Energy Sciences, Tokyo Institute of Technology, Yokohama 226-8502, Japan*
[5]*Center for Nuclear Study, University of Tokyo, Wako, Saitama 351-0198, Japan*
[6]*Department of Physics, Kyushu University, Fukuoka 812-8581, Japan*
[7]*Department of Physics, University of Surrey, Guildford, GU2 7XH, United Kingdom*
(Received 7 January 2008; published 24 April 2008)

Modest spin states in neutron-rich $^{187}$W have been populated by using a $^{186}$W($^{18}$O,$^{17}$O) one-neutron transfer reaction. Negative-parity bands previously known are extended to higher spin, and two positive-parity bands are newly identified. Configurations based on $\nu$ i$_{13/2}$ orbitals are assigned to these bands from an analysis of the level energy systematics as well as the g factors derived from in-band branching ratios.

DOI: 10.1103/PhysRevC.77.047303 PACS number(s): 23.20.Lv, 25.70.Hi, 27.70.+q

The deformed nucleus $^{187}$W is located on the neutron-rich side of the nuclear valley of stability and therefore it is difficult to study its near-yrast structure owing to lack of a suitable reaction mechanism. Low-lying levels in $^{187}$W are known from neutron capture [1–3] and $(d, p)$ transfer reaction studies [3–6]. In addition, the $K^{\pi} = 11/2^{+}$, $T_{1/2} = 1.55$ $\mu$s isomer at 411 keV has been identified in our previous study by using a deep inelastic reaction [7]. In the present work, we employed an in-beam $\gamma$-ray spectroscopic method to investigate higher spin states of $^{187}$W populated in an $^{18}$O-induced one-neutron transfer reaction. This type of experimental technique is effective for the investigation of near-yrast structure in moderately neutron rich nuclei [8–13].

The experiment was carried out at the tandem accelerator facility, JAEA, Tokai [14]. Excited states of $^{187}$W were populated by a one-neutron transfer reaction of $^{186}$W($^{18}$O,$^{17}$O). A self-supporting target of $^{186}$W enriched to 98.2% was bombarded by an 180-MeV $^{18}$O beam. The target was made of two stacked 450 $\mu$g/cm$^2$ metallic foils, which are thick enough to stop target-like nuclei inside the target. Scattered light ions were detected by four sets of surface-barrier Si $\Delta E$-$E$ detectors. The $\gamma$ rays emitted from the residual nuclei were measured by seven HP-Ge detectors in coincidence with the outgoing ions. Four of these detectors with relative efficiency of 60% were arranged symmetrically in a plane perpendicular to the beam axis at a distance of 6 cm from the target. Two of these four Ge detectors and two of the Si $\Delta E$-$E$ detectors were placed in a horizontal plane including the beam axis, while the other two Ge detectors and two Si $\Delta E$-$E$ detectors were in a vertical plane. This setup allows us to extract $\gamma$-ray anisotropies for determination of transition multipole orders. The remaining three Ge detectors with relative efficiency of 30–40% were installed between the four Ge detectors. The energy and efficiency calibration of the Ge detectors was made by using standard $\gamma$-ray sources of $^{133}$Ba and $^{152}$Eu. The details of the experimental setup are described in Ref. [12].

An $E$-$\Delta E$ plot for outgoing ions measured by the Si detectors is shown in Fig. 1. The ions are clearly separated by mass and atomic numbers. The energies of ions are calibrated by assuming that the most intense peak in the $E$-$\Delta E$ plot corresponds to elastically scattered events of $^{18}$O ions entering at the center of the each Si detector. The dashed line in Fig. 1 represents calculated energy losses for $^{17}$O. Figure 2 shows $\gamma$-ray energy spectra gated on $^{17}$O ions with the different kinetic energy windows shown in Fig. 1. In Figs. 2(a) and 2(b), $\gamma$-ray peaks from $^{187}$W and $^{186}$W, respectively, are observed. The $^{186}$W nucleus can be produced by one-neutron evaporation from $^{187}$W, when the compound-like $^{187}$W formed in the one-neutron transfer reaction is excited above the neutron separation energy of 5.5 MeV. Thus, the higher energy $^{17}$O gate is used for the present analysis.

Figure 3 shows a level scheme for $^{187}$W deduced from the present experimental data. The spin and parity assignments of the levels are based on $\gamma$-ray feeding pattern as well as $\gamma$-ray anisotropy [8,9] with respect to the reaction plane. Table I summarizes energies and relative intensities of $\gamma$-ray transitions observed in $^{187}$W. The intensities are extracted

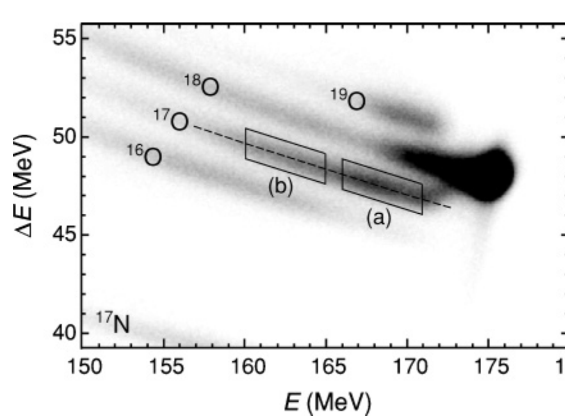


FIG. 1. $E$-$\Delta E$ plot for ions measured by the Si detectors. The dashed line shows calculated energy losses for $^{17}$O. The enclosed areas represent gate windows with kinetic energies of (a) 166–171 MeV and (b) 160–165 MeV; see Fig. 2.

 

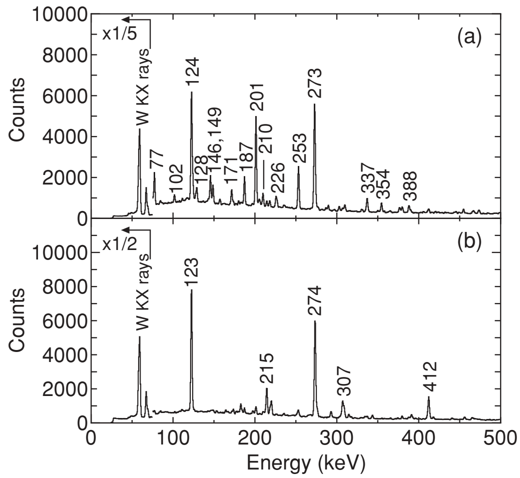


FIG. 2. $\gamma$-ray energy spectra gated on $^{17}$O ions with kinetic energies of (a) 166–171 MeV and (b) 160–165 MeV, corresponding to the gate windows (a) and (b) shown in Fig. 1. The $\gamma$ rays assigned to (a) $^{187}$W and (b) $^{186}$W are labeled in units of keV.

from $\gamma$-$\gamma$ coincidence data. Low-lying levels of this nucleus have been studied via neutron capture [1–3], $(d, p)$ transfer reactions [3–6], and deep-inelastic reactions [7]. The ground-state band, based on the $3/2^-[512]$ Nilsson configuration, was previously identified up to a spin and parity of $I^\pi = 9/2^-$ [1,3]. The present data extend this band up to $I^\pi = (21/2^-)$ with firm assignments made up to $I^\pi = 15/2^-$. The $1/2^-[510]$ band was known earlier up to an $I^\pi = 9/2^-$ level at 599 keV [3]. In the present work the band members up to $I^\pi = (19/2^-)$ have been identified. The measured excitation energy of the $I^\pi = 9/2^-$ state at 613 keV is different from the previous assignment. In the $(d, p)$ transfer reaction [3], the 599-keV level was populated with a cross section of 38(5) $\mu$b, which was larger than the expectation for the $9/2^-$ state. As shown later, the $I^\pi = 13/2^+$ state of the $11/2^+[615]$ band is observed at 597 keV, which is close to 599 keV. This reveals the strong population of the 599-keV level in the $(d, p)$ reaction owing to the underlying $i_{13/2}$ component. Interband transitions to the $3/2^-[512]$ band members indicate a mixing between these bands.

The $7/2^-[503]$ band is built on an isomeric state with a half-life of $T_{1/2} = 5$ ns at 350 keV. The isomeric bandhead decays to the $I^\pi = 5/2^-$ and $7/2^-$ members of the $3/2^-[512]$ band. The observation of cascade $M1(+E2)$ transitions of 171 and 206 keV, and a corresponding cross-over $E2$ transition of 377 keV, allows us to place the $I^\pi = 11/2^-$ band member at 727 keV instead of the previous tentative placement at 723 keV [3]. Thus, the present data extend this band up to an $I^\pi = (15/2^-)$ level at 1229 keV. A level at 639 keV

TABLE I. Energies $E_\gamma$ and relative intensities $I_\gamma$ of the $\gamma$-ray transitions observed in $^{187}$W.

| $E_\gamma$ (keV) | $I_\gamma$ | $E_\gamma$ (keV) | $I_\gamma$ |
|---|---|---|---|
| (14) | | 286.8(5) | <1 |
| 46.0(5) | 39(5) | 289.5(1) | 40(4) |
| (59) | | 303.1(2) | 27(8) |
| 77.2(1) | 137(14) | 310.1(1) | 39(4) |
| (98) | | 337.0(1) | 208(10) |
| 101.8(1) | 53(4) | 354.2(2) | 88(19) |
| 124.1(1) | 275(20) | 364.7(1) | 21(2) |
| 127.6(1) | 27(11) | 377.0(2) | 46(7) |
| 128.9(1) | 56(5) | 380.0(1) | 94(6) |
| 129.1(2) | 21(4) | 388.0(1) | 275(50) |
| 145.7(1) | 137(14) | 405.1(2) | 55(11) |
| 148.8(1) | 126(6) | 407.3(2) | 7(1) |
| 157.3(2) | 19(3) | 410.8(5) | ∼1 |
| 171.4(1) | 121(6) | 443.3(2) | 17(3) |
| 180.1(1) | 46(3) | 445.7(2) | 82(5) |
| 187.2(1) | 890(80) | 450.0(2) | 8(2) |
| 200.7(2) | 23(3) | 458.1(1) | 27(5) |
| 201.3(1) | 962(124) | 466.3(1) | 27(3) |
| 205.7(1) | 55(4) | 468.0(1) | 31(3) |
| 209.8(1) | 139(7) | 496.3(2) | 14(2) |
| 218.2(1) | 128(7) | 498.5(1) | 21(3) |
| 225.7(1) | 69(10) | 501.5(2) | 7(2) |
| 227.0(1) | 25(5) | 502.8(2) | 8(2) |
| 230.2(5) | ∼1 | 550.3(2) | 10(2) |
| 235.7(1) | 27(3) | 568.7(1) | 18(6) |
| 236.6(2) | 16(2) | (587) | |
| 239.5(1) | 38(8) | 590.5(1) | 2(1) |
| 245.1(2) | 7(1) | (619) | ∼1 |
| 253.2(1) | 410(32) | 694.9(2) | 8(2) |
| 272.7(1) | 1000(50) | 777.7(2) | 2(1) |
| 282.5(2) | 8(2) | | |

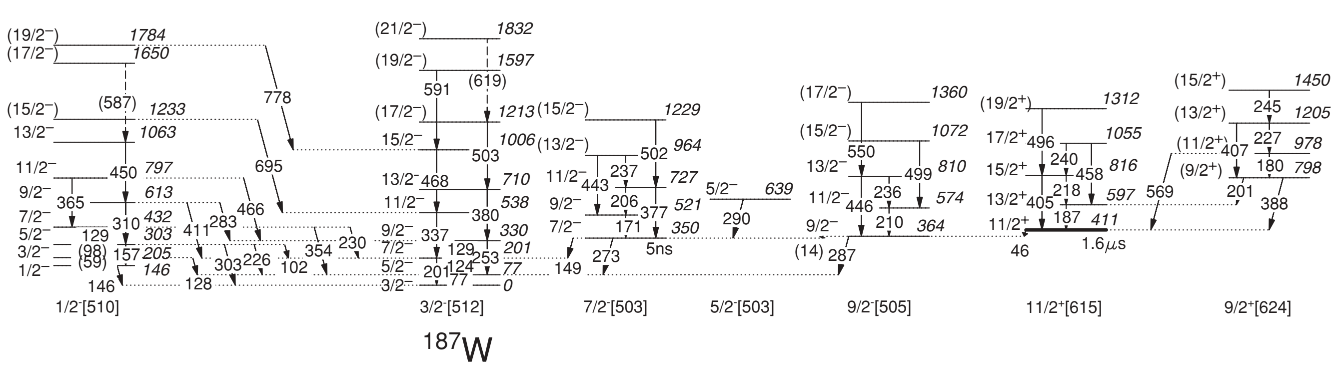


FIG. 3. A proposed level scheme of $^{187}$W. The Nilsson configurations are shown. The $\gamma$-ray and level energies are shown in units of keV.

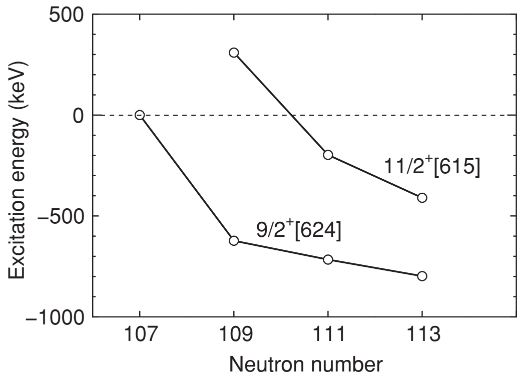


FIG. 4. Bandhead energies of the positive-parity Nilsson orbitals in W isotopes. Points at positive (negative) states indicate particle (hole) states.

decaying to the $7/2^-[503]$ band via a 290-keV transition was previously assigned as the $5/2^-[503]$ bandhead [3,5], and this is confirmed in the present work.

The $9/2^-[505]$ bandhead at 364 keV decays to both the $3/2^-[512]$ and $7/2^-[503]$ bands [3,7]. An $I^\pi = 11/2^-$ level at 574 keV tentatively placed in this band [3] is confirmed. The present data extend this band to higher spin states.

A 411-keV isomer with $T_{1/2} = 1.6$ $\mu$s, based on the $11/2^+[615]$ Nilsson configuration, was observed in our previous study [7]. This isomer decays to the $I^\pi = 9/2^-$ level at 364 keV via a 46-keV transition. In the present work, two rotational bands are identified above the isomer in the analysis of delayed coincidences across the isomer. Levels at 597, 816, 1055, and 1312 keV form a strongly coupled rotational band built on the isomer itself. Three $\gamma$-ray transitions of 201, 388, and 569 keV link a newly observed structure built on a 798-keV state to the low-lying members of the $11/2^+[615]$ band. The $\gamma$-ray anisotropy data for the 388- and 569-keV transitions are consistent with the assignments of $I = (9/2$ or $11/2)$ and $(11/2$ or $13/2)$ for the 798- and 978-keV levels, respectively. Since these levels decay only to the $11/2^+[615]$ band, the $K^\pi = 9/2^+$ assignment is preferred for this newly observed band.

The $9/2^+[624]$ and $11/2^+[615]$ orbitals are known for the lighter W isotopes of $^{181}$W, $^{183}$W and $^{185}$W [15]. In Fig. 4 excitation energies for these orbitals are compared with the corresponding levels in $^{187}$W. The 798-keV level in $^{187}$W lies on the systematics for the $9/2^+[624]$ orbitals. The $M1$ transition energies of 180, 227, and 245 keV in the $K^\pi = 9/2^+$ band are also consistent with the systematics of $K^\pi = 9/2^+[624]$ bands in the region [15] [i.e., increasing the $M1$ transition energy for heavier (less-deformed) W isotopes].

To confirm the Nilsson configuration, in-band branching ratios are examined. Experimental $|g_K - g_R|$ values are evaluated with the rotational model expressions [16]. The quadrupole moment of $Q_0 = 6.8$ $e$ b are chosen as the average

TABLE II. Experimental $|g_K - g_R|$ values deduced from the branching ratios $\lambda$ for the bands in $^{187}$W compared with the corresponding calculated values.

| $K^\pi$ | $I_i$ | $E_2$ (keV) | $E_1$ (keV) | $\lambda$ | $\lvert g_K^{exp} - g_R\rvert$ | $\lvert g_K^{cal} - g_R\rvert$ [a] |
|---|---|---|---|---|---|---|
| $3/2^-$ | 7/2 | 201.3 | 124.1 | 3.5(5) | 0.25(3) | 0.24(5) |
| | 9/2 | 253.2 | 129.1 | 20(4) | 0.21(4) | 0.24(5) |
| $7/2^-$ | 11/2 | 377.0 | 205.7 | 0.84(14) | 0.50(10) | 0.64(5) |
| | 13/2 | 443.3 | 236.6 | 1.1(3) | 0.68(9) | 0.64(5) |
| $9/2^-$ | 13/2 | 445.7 | 235.6 | 3.0(4) | 0.12(4) | 0.03(5) |
| $9/2^+$ | 13/2 | 407.3 | 226.9 | 0.28(8) | 0.68(11) | 0.53(5) |
| $11/2^+$ | 15/2 | 405.1 | 218.2 | 0.43(9) | 0.42(5) | 0.48(5) |
| | 17/2 | 458.1 | 239.5 | 0.71(20) | 0.51(8) | 0.48(5) |

[a] $g_R = 0.30(5)$ is used.

of the values for $^{183}$W [17] and $^{185}$Ta [18]. Table II compares the experimental and calculated $g_K$ factors for the bands observed in $^{187}$W. For each band, the experimentally derived $g_K$ factors agree, within the uncertainties, with the calculated values for the proposed one-quasiparticle configurations. The results support the $9/2^+[624]$ and $11/2^+[615]$ assignment for the newly observed bands built above the isomer.

A self-consistent Hartree-Fock-Bogoliubov cranking calculation of the type described in Ref. [19] has been performed for the $K^\pi = 3/2^-$ band in $^{187}$W. The spherical Nilsson Hamiltonian was chosen for the one-body part in the cranking Hamiltonian and the $P + Q.Q$ force for the two-body interaction. The model space consists of two-plus-two major shells both for protons ($N = 4$ and 5) and neutrons ($N = 5$ and 6). The result of the present calculation indicates an almost constant deformation of $\beta \sim 0.20$ for the states up to $I^\pi = 21/2^-$. In contrast, the triaxial deformation gradually evolves, as the total angular momentum increases, from $\gamma = 0.6^\circ$ at $I^\pi = 3/2^-$ to $\gamma = 14^\circ$ at $I^\pi = 21/2^-$. This is consistent with the results obtained in our previous studies for even-even W isotopes [12]. Slightly triaxial deformation ($\gamma = 6.6^\circ$) is predicted at $I^\pi = 10^+$ for the ground-state band in $^{188}$W. Note that the present $\gamma$ parametrization follows the Hill-Wheeler definition [20], which has the opposite sign to that of the Lund convention.

In summary, the near-yrast states of neutron-rich $^{187}$W have been populated by using an $^{18}$O-induced one-neutron transfer reaction. Two positive-parity bands are identified and assigned $\nu\, i_{13/2}$ Nilsson configuration. The result of a self-consistent cranking calculation implies that the ground-state band of $^{187}$W maintains near axially symmetric shapes $|\gamma| \lesssim 15^\circ$ up to $I^\pi = 21/2^-$.

We thank G. Sletten for the preparation of the $^{186}$W target and the staff of the JAEA tandem accelerator facility for providing the $^{18}$O beam.

[1] R. F. Casten, D. Breitig, O. A. Wasson, K. Rimawi, and R. E. Chrien, Nucl. Phys. **A228**, 493 (1974).

[2] A. M. Bruce, D. Hicks, and D. D. Warner, Nucl. Phys. **A465**, 221 (1987).

[3] V. Bondarenko, A. V. Afanasjev, T. von Egidy, L. Simonova, J. Berzin, I. Kuvaga, W. Schauer, J. Ott, P. Prokofjevs, R. Georgii, M. Kessler, T. Körbitz, and W. Schott, Nucl. Phys. **A619**, 1 (1997).

[4] J. R. Erskine, Phys. Rev. **138**, 66 (1965).

[5] R. F. Casten, P. Kleinheinz, P. J. Daly, and B. Elbek, K. Dan. Vidensk. Selsk., Mat. Fys. Medd. **38**, 13 (1972).

[6] R. F. Casten, P. W. Keaton, and G. P. Lawrence, Phys. Rev. C **7**, 1016 (1973).

[7] T. Shizuma, T. Hayakawa, S. Mitarai, T. Morikawa, and T. Ishii, Phys. Rev. C **71**, 067301 (2005).

[8] T. Ishii, S. Shigematsu, M. Asai, A. Makishima, M. Matsuda, J. Kaneko, I. Hossain, S. Ichikawa, T. Kohno, and M. Ogawa, Phys. Rev. C **72**, 021301(R) (2005).

[9] T. Ishii, S. Shigematsu, H. Makii, M. Asai, K. Tsukada, A. Toyoshima, M. Matsuda, A. Makishima, T. Shizuma, J. Kaneko, I. Hossain, H. Toume, M. Ohara, S. Ichikawa, T. Kohno, and M. Ogawa, J. Phys. Soc. Jpn. **75**, 043201 (2006).

[10] T. Ishii, H. Makii, M. Asai, H. Koura, S. Shigematsu, K. Tsukada, A. Toyoshima, M. Matsuda, A. Makishima, J. Kaneko, H. Toume, I. Hossain, T. Shizuma, S. Ichikawa, T. Kohno, and M. Ogawa, Phys. Rev. C **76**, 011303(R) (2007).

[11] H. Makii, T. Ishii, M. Asai, K. Tsukada, A. Toyoshima, M. Matsuda, A. Makishima, J. Kaneko, H. Toume, S. Ichikawa, S. Shigematsu, T. Kohno, and M. Ogawa, Phys. Rev. C **76**, 061301(R) (2007).

[12] T. Shizuma, T. Ishii, H. Makii, T. Hayakawa, S. Shigematsu, M. Matsuda, E. Ideguchi, Y. Zheng, M. Liu, T. Morikawa, P. M. Walker, and M. Oi, Eur. Phys. J. A **30**, 391 (2006).

[13] T. Shizuma, T. Ishii, H. Makii, T. Hayakawa, S. Shigematsu, M. Matsuda, E. Ideguchi, Y. Zheng, M. Liu, and T. Morikawa, Eur. Phys. J. A **34**, 1 (2007).

[14] S. Takeuchi, T. Ishii, M. Matsuda, Y. Zhang, and T. Yoshida, Nucl. Instrum. Methods Phys. Res. A **382**, 153 (1996).

[15] ENSDF, NNDC Online Data Service, ENSDF database, http://www.nndc.bnl.gov/nndc/ensdf/.

[16] A. Bohr and B. R. Mottelson, *Nuclear Structure*, Vol. 2 (Benjamin, Reading, MA, 1975).

[17] T. R. Saitoh, N. Saitoh-Hashimoto, G. Sletten, R. A. Bark, M. Bergström, P. Regan, S. Tömaänen, P. G. Varmette, P. M. Walker, and C. Wheldon, Nucl. Phys. **A669**, 381 (2000).

[18] C. Wheldon, P. M. Walker, R. D'Alarcao, P. Chowdhury, C. J. Pearson, E. H. Seabury, I. Ahmad, M. P. Carpenter, D. M. Cullen, G. Hackman, R. V. F. Janssens, T. L. Khoo, D. Nisius, and P. Reiter, Eur. Phys. A **5**, 353 (1999).

[19] M. Oi, Phys. Rev. C **76**, 044308 (2007).

[20] D. L. Hill and J. A. Wheeler, Phys. Rev. **89**, 1102 (1953).